JOC Article
pubs.acs.org/joc

Competitive Enantiodifferentiating Anti-Markovnikov Photoaddition of Water and Methanol to 1,1-Diphenylpropene Using A Sensitizing Cyclodextrin Host

Gaku Fukuhara, Tadashi Mori, and Yoshihisa Inoue*

Department of Applied Chemistry, Osaka University, 2-1Yamada-oka, Suita 565-0871, Japan

inoue@chem.eng.osaka-u.ac.jp

Received June 16, 2009

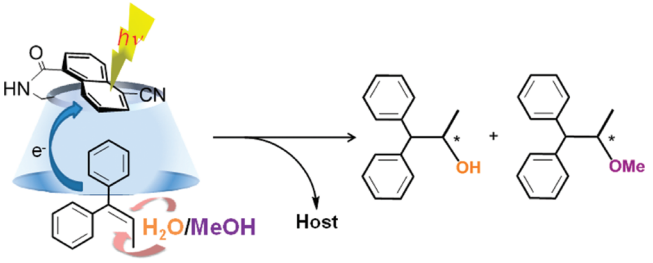

UV−vis, circular dichroism (CD), fluorescence, and NMR spectral studies on the self-inclusion behavior of a newly synthesized sensitizing host, 6-(5-cyanonaphthyl-1-carboamido)-6-deoxy-β-cyclodextrin (**1**), showed that the appended naphthalene moiety of **1** perches laterally on the cyclodextrin rim in aqueous methanol but is shallowly included and somewhat tilted in its own cavity in water. UV−vis and CD spectral examinations of the complexation of guest substrate 1,1-diphenylpropene (**DPP**) with host **1** revealed the formation of a stoichiometric 1:1 complex of **DPP** with **1**. The naphthyl fluorescence of **1** was efficiently quenched by the addition of **DPP** in aqueous solutions of low methanol contents (≤25%) but was less efficiently quenched in more hydrophobic solvents (≥50% methanol), where the fluorophore is not included in the cavity and allows the external attack of **DPP** to form an exciplex in the bulk solution. Upon irradiation in aqueous solutions of different methanol contents, competitive photoaddition of water and methanol to **DPP** occurred to give chiral water adduct **3** and methanol adduct **4**, favoring the latter product by a factor of 2.5 due to the higher nucleophilicity of methanol. The enantiomeric excess (ee) values of the photoadducts were generally low in highly methanolic solutions, but was greatly improved by increasing the water content to reach 18% ee for **3** and 13% ee for **4** in 10% methanol solution at −10 °C. Interestingly, the ee of methanol adduct **4** was consistently lower than that of water adduct **3** particularly in water-rich solvents, revealing that the product's ee is not a simple thermodynamic function of the enantioface-selectivity upon complexation of **DPP** by chiral host **1** but also kinetically controlled by the subsequent photoinduced enantioface-differentiating nucleophilic attack of water and methanol to radical cationic **DPP** generated photochemically. Compatible with this mechanism, the compensation plot of the differential activation enthalpy versus entropy, which were obtained from the van't Hoff analysis of the temperature-dependent ee's obtained in aqueous solutions of varying methanol contents, gave an excellent straight line for water adduct **3** but an unprecedented bent plot for methanol adduct **4**, indicating a switching of the mechanism in between 35 and 50% methanol solution. By using high pressure, low temperature, and/or added salt, the ee of water adduct **3** was further enhanced to 24−26%.

Introduction

Photochirogenesis,[1] which enables us to access the thermally forbidden routes to chiral compounds, is an attractive alternative to the conventional asymmetric syntheses using chiral catalysts or enzymes.[2−4] One of the most intriguing features of photochirogenesis is the critical control of enantioselectivity, including the switching of chiral sense, of

Published on Web 08/11/2009 DOI: 10.1021/jo9012628

photoproduct through the manipulation of a variety of entropy-related environmental variants such as temperature,[5] pressure,[6] and solvation,[7] which provides us with a unique, versatile tool for multidimensionally optimizing a photochirogenic reaction without using a harsh condition.[8] More importantly, these observations unambiguously revealed the essential roles of the entropy played in the enantiodifferentiating step of photochirogenic reaction.

From the entropic point of view, supramolecular hosts are of particular interest,[9,10] possessing a highly ordered, inherently low entropic, cavity for confining a guest. Thus, several groups have exploited a wide range of chiral supramolecular hosts for photochirogenesis, which include native and modified cyclodextrins,[11,12] biomolecules,[13] chirally modified zeolites,[14] hydrogen-bonding templates,[15] and chiral nanoporous materials.[16] In the enantiodifferentiating photoisomerization of (*Z*)-cyclooctene included and sensitized by β-cyclodextrin derivatives with a tethered sensitizing group,[12b,p] (*E*)-isomer was obtained in 46% enantiomeric excess (ee), which is significantly higher than the practically zero ee obtained upon direct excitation of (*Z*)-cyclooctene included in native β-cyclodextrin.[11b] Interestingly, the product's ee was independent of the temperature or solvent composition used, but was nicely correlated with the host occupancy, suggesting an insignificant role of entropy in the supramolecular photochirogenesis as was the case with the photochirogenesis in rigid nanopores of zeolites.[14] These findings may suggest that the supramolecular environment is not suitable for dynamically controlling a photochirogenic process, thus limiting the scope of the supramolecular approach. However, we have demonstrated more recently that the product's ee and chiral sense become susceptible to such entropy-related variants as temperature and solvent in the enantiodifferentiating photoisomerization mediated by permethylated 6-*O*-aroylcyclodextrins, for which the flexible permethylated cyclodextrin skeleton[17] is likely to be responsible.[12g,k] This contrasting behavior allows us to further

(1) For reviews, see: (a) Rau, H. *Chem. Rev.* **1983**, *83*, 535. (b) Inoue, Y. *Chem. Rev.* **1992**, *92*, 741. (c) Pete, J. P. *Adv. Photochem.* **1996**, *21*, 135. (d) Everitt, S. R. L.; Inoue, Y. In *Molecular and Supramolecular Photochemistry*; Ramamurthy, V., Schanze, K. S., Eds.; Marcel Dekker: New York, 1999. (e) Griesbeck, A. G.; Meierhenrich, U. J. *Angew. Chem., Int. Ed.* **2002**, *41*, 3147. (f) Inoue, Y., Ramamurthy, V., Eds. *Chiral Photochemistry*; Marcel Dekker: New York, 2004. (g) Inoue, Y. *Nature* **2005**, *436*, 1099. (h) Müller, C.; Bach, T. *Aust. J. Chem.* **2008**, *61*, 537.

(2) Hoffmann, N. *Chem. Rev.* **2008**, *108*, 1052.

(3) Nobel Lectures, see: (a) Knowles, W. S. *Angew. Chem., Int. Ed.* **2002**, *41*, 1998. (b) Noyori, R. *Angew. Chem., Int. Ed.* **2002**, *41*, 2008. (c) Sharpless, K. B. *Angew. Chem., Int. Ed.* **2002**, *41*, 2024.

(4) Hammond, G. S.; Cole, R. S. *J. Am. Chem. Soc.* **1965**, *87*, 3256.

(5) (a) Inoue, Y.; Yokoyama, T.; Yamasaki, N.; Tai, A. *J. Am. Chem. Soc.* **1989**, *111*, 6480. (b) Inoue, Y.; Yokoyama, T.; Yamasaki, N.; Tai, A. *Nature* **1989**, *341*, 225. (c) Inoue, Y.; Yamasaki, N.; Yokoyama, T.; Tai, A. *J. Org. Chem.* **1992**, *57*, 1332. (d) Inoue, Y.; Yamasaki, N.; Yokoyama, T.; Tai, A. *J. Org. Chem.* **1993**, *58*, 1011.

(6) (a) Inoue, Y.; Matsushima, E.; Wada, T. *J. Am. Chem. Soc.* **1998**, *120*, 10687. (b) Kaneda, M.; Asaoka, S.; Ikeda, H.; Mori, T.; Wada, T.; Inoue, Y. *Chem. Commun.* **2002**, 1272. (c) Kaneda, M.; Nakamura, A.; Asaoka, S.; Ikeda, H.; Mori, T.; Wada, T.; Inoue, Y. *Org. Biomol. Chem.* **2003**, *1*, 4435.

(7) Inoue, Y.; Ikeda, H.; Kaneda, M.; Sumimura, T.; Everitt, S. R. L.; Wada, T. *J. Am. Chem. Soc.* **2000**, *122*, 406.

(8) (a) Inoue, Y.; Wada, T.; Asaoka, S.; Sato, H.; Pete, J.-P. *Chem. Commun.* **2000**, 251. (b) Inoue, Y.; Sugahara, N.; Wada, T. *Pure Appl. Chem.* **2001**, *73*, 475.

(9) (a) Whiteside, G. M. *Sci. Am.* **1995**, *273*, 114. (b) Lehn, J.-M. *Supramol. Chem.*; VCH: Weinheim, Germany, 1995. (c) Philip, D.; Stoddart, J. F. *Angew. Chem., Int. Ed. Engl.* **1996**, *35*, 154. (d) Fredericks, J. R.; Hamilton, A. D. In *Comprehensive Supramolecular Chemistry*; Atwood, J. L., Davies, J. E. D., MacNicol, D. D., Vögtle, F., Eds.; Pergamon/Elsevier: Oxford, 1996. (e) Hartley, J. H.; James, T. D.; Ward, C. J. *J. Chem. Soc., Perkin Trans. 1* **2000**, 3155. (f) *Molecular Machines Special Issue; Acc. Chem. Res.* **2001**, *34*. 409. (g) Reinhoudt, D. N.; Crego-Calama, M. *Science* **2002**, *295*, 2403. (h) Shinkai, S.; Takeuchi, M. *Bull. Chem. Soc. Jpn.* **2005**, *78*, 40. (i) Fukuhara, G.; Madenci, S.; Polkowska, J.; Bastkowski, F.; Klärner, F.-G.; Origane, Y.; Kaneda, M.; Mori, T.; Wada, T.; Inoue, Y. *Chem.*−*Eur. J.* **2007**, *13*, 2473. (j) Fukuhara, G.; Klärner, F.-G.; Mori, T.; Wada, T.; Inoue, Y. *Photochem. Photobiol. Sci.* **2008**, *7*, 1493 and references therein.

(10) (a) Inoue, Y., Gokel, G. W., Eds. *Cation Binding by Macrocycles*; Marcel Dekker: New York, 1990. (b) Inoue, Y.; Hakushi, T.; Liu, Y.; Tong, L.-H.; Shen, B.-J.; Jin, D.-S. *J. Am. Chem. Soc.* **1993**, *115*, 475. (c) Inoue, Y.; Liu, Y.; Tong, L.-H.; Shen, B.-J.; Jin, D.-S. *J. Am. Chem. Soc.* **1993**, *115*, 10637. (d) Inoue, Y., Wada, T., Gokel, G. W., Eds. *Advances in Supramolecular Chemistry*; JAI Press: Greenwich, C T, 1997. (e) Rekharsky, M. V.; Inoue, Y. *Chem. Rev.* **1998**, *98*, 1875. (f) Rekharsky, M. V.; Inoue, Y. In *Cyclodextrins and Their Complexes*; Helena, D.; , Ed.; Wiley-VCH: Weinheim, Germany, 2008; pp 199−230.

(11) (a) Rao, V. P.; Turro, N. J. *Tetrahedron Lett.* **1989**, *30*, 4641. (b) Inoue, Y.; Kosaka, S.; Matsumoto, K.; Tsuneishi, H.; Hakushi, T.; Tai, A.; Nakagawa, K.; Tong, L.-H. *J. Photochem. Photobiol., A: Chem.* **1993**, *71*, 61. (c) Koodanjeri, S.; Joy, A.; Ramamurthy, V. *Tetrahedron* **2000**, *56*, 7003. (d) Vízvárdi, K.; Desmet, K.; Luyten, I.; Sandra, P.; Hoornaert, G.; Eycken, E. V. *Org. Lett.* **2001**, *3*, 1173. (e) Koodanjeri, S.; Joy, A.; Ramamurthy, V. *Tetrahedron Lett.* **2002**, *43*, 9229. (f) Shailaja, J.; Karthikeyan, S.; Ramamurthy, V. *Tetrahedron Lett.* **2002**, *43*, 9335. (g) Nakamura, A.; Inoue, Y. *J. Am. Chem. Soc.* **2003**, *125*, 966. (h) Furutani, A.; Katayama, K.; Ueshima, Y.; Ogura, M.; Tobe, Y.; Kurosawa, H.; Tsutsumi, K.; Morimoto, T.; Kakiuchi, K. *Chirality* **2006**, *18*, 217.

(12) (a) Inoue, Y.; Dong, F.; Yamamoto, K.; Tong, L.-H.; Tsuneishi, H.; Hakushi, T.; Tai, A. *J. Am. Chem. Soc.* **1995**, *117*, 11033. (b) Inoue, Y.; Wada, T.; Sugahara, N.; Yamamoto, K.; Kimura, K.; Tong, L.-H.; Gao, X.-M.; Hou, Z.-J.; Liu, Y. *J. Org. Chem.* **2000**, *65*, 8041. (c) Gao, Y.; Inoue, M.; Wada, T.; Inoue, Y. *J. Incl. Phenom. Macrocycl. Chem.* **2004**, *50*, 111. (d) Ikeda, H.; Nihei, T.; Ueno, A. *J. Org. Chem.* **2005**, *70*, 1237. (e) Nakamura, A.; Inoue, Y. *J. Am. Chem. Soc.* **2005**, *127*, 5338. (f) Yang, C.; Fukuhara, G.; Nakamura, A.; Origane, Y.; Fujita, K.; Yuan, D.-Q.; Mori, T.; Wada, T.; Inoue, Y. *J. Photochem. Photobiol., A: Chem.* **2005**, *173*, 375. (g) Fukuhara, G.; Mori, T.; Wada, T.; Inoue, Y. *Chem. Commun.* **2005**, 4199. (h) Yang, C.; Nakamura, A.; Fukuhara, G.; Origane, Y.; Mori, T.; Wada, T.; Inoue, Y. *J. Org. Chem.* **2006**, *71*, 3126. (i) Fukuhara, G.; Mori, T.; Wada, T.; Inoue, Y. *Chem. Commun.* **2006**, 1712. (j) Yang, C.; Nakamura, A.; Wada, T.; Inoue, Y. *Org. Lett.* **2006**, *8*, 3005. (k) Fukuhara, G.; Mori, T.; Wada, T.; Inoue, Y. *J. Org. Chem.* **2006**, *71*, 8233. (l) Yang, C.; Mori, T.; Wada, T.; Inoue, Y. *New J. Chem.* **2007**, *31*, 697. (m) Yang, C.; Nishijima, M.; Nakamura, A.; Mori, T.; Wada, T.; Inoue, Y. *Tetrahedron Lett.* **2007**, *48*, 4357. (n) Lu, R.; Yang, C.; Cao, Y.; Wang, Z.; Wada, T.; Jiao, W.; Mori, T.; Inoue, Y. *Chem. Commun.* **2008**, 374. (o) Yang, C.; Mori, T.; Inoue, Y. *J. Org. Chem.* **2008**, *73*, 5786. (p) Lu, R.; Yang, C.; Cao, Y.; Tong, L.; Jiao, W.; Wada, T.; Wang, Z.; Mori, T.; Inoue, Y. *J. Org. Chem.* **2008**, *73*, 7695. (q) Qiu, H.; Yang, C.; Inoue, Y.; Che, S. *Org. Lett.* **2009**, *11*, 1793.

(13) (a) Wada, T.; Sugahara, N.; Kawano, M.; Inoue, Y. *Chem. Lett.* **2000**, 1174. (b) Wada, T.; Nishijima, M.; Fujisawa, T.; Sugahara, N.; Mori, T.; Nakamura, A.; Inoue, Y. *J. Am. Chem. Soc.* **2003**, *125*, 7492. (c) Lhiaubet-Vallet, V.; Encinas, S.; Miranda, M. A. *J. Am. Chem. Soc.* **2005**, *127*, 12774. (d) Nishijima, M.; Pace, T. C. S.; Nakamura, A.; Mori, T.; Wada, T.; Bohne, C.; Inoue, Y. *J. Org. Chem.* **2007**, *72*, 2707. (e) Nishijima, M.; Wada, T.; Mori, T.; Pace, T. C. S.; Bohne, C.; Inoue, Y. *J. Am. Chem. Soc.* **2007**, *129*, 3478.

(14) (a) Ramamurthy, V. *J. Chem. Soc., Chem. Commun.* **1998**, 1379. (b) Joy, A.; Scheffer, R.; Ramamurthy, V. *Org. Lett.* **2000**, *2*, 119. (c) Turro, N. J. *Acc. Chem. Res.* **2000**, *33*, 637. (d) Wada, T.; Shikimi, M.; Inoue, Y.; Lem, G.; Turro, N. J. *Chem. Commun.* **2001**, 1864. (e) Chong, K. C. W.; Sivaguru, J.; Shichi, T.; Yoshimi, Y.; Ramamurthy, V.; Scheffer, J. R. *J. Am. Chem. Soc.* **2002**, *124*, 2858. (f) Sivaguru, J.; Natarajan, A.; Kaanumalle, L. S.; Shailaja, J.; Uppili, S.; Joy, A.; Ramamurthy, V. *Acc. Chem. Res.* **2003**, *36*, 509. (g) Sivaguru, J.; Poon, T.; Franz, R.; Jockusch, S.; Adam, W.; Turro, N. J. *J. Am. Chem. Soc.* **2004**, *126*, 10816. (h) Sivaguru, J.; Saito, H.; Solomon, M. R.; Kaanumalle, L. S.; Roon, T.; Franz, R.; Jockusch, S.; Adam, W.; Ramamurthy, V.; Inoue, Y.; Turro, N. J. *Photochem. Photobiol. Sci.* **2006**, *82*, 123. (i) Sivasubramanian, K.; Kaanumalle, L. S.; Uppili, S.; Ramamurthy, V. *Org. Biomol. Chem.* **2007**, *5*, 1569.

(15) (a) Grosch, B.; Orlebar, C. N.; Herdtweck, E.; Massa, W.; Bach, T. *Angew. Chem., Int. Ed.* **2003**, *42*, 3693. (b) Grosch, B.; Orlebar, C. N.; Herdtweck, E.; Kaneda, M.; Wada, T.; Inoue, Y.; Bach, T. *Chem.*−*Eur. J.* **2004**, *10*, 2179. (c) Aechtner, T.; Dressel, M.; Bach, T. *Angew. Chem., Int. Ed.* **2004**, *43*, 5849. (d) Bauer, A.; Weskamper, F.; Grimme, S.; Bach, T. *Nature* **2005**, 1139. (e) Mizoguchi, J.; Kawanami, Y.; Wada, T.; Kodama, K.; Anzai, K.; Yanagi, T.; Inoue, Y. *Org. Lett.* **2006**, *8*, 6051.

(16) Gao, Y.; Wada, T.; Yang, K.; Kim, K.; Inoue, Y. *Chirality* **2005**, *17*, 19.

(17) (a) Jullien, L.; Canceill, J.; Lacombe, L.; Lehn, J.-M. *J. Chem. Soc., Perkin Trans. 2* **1994**, 989. (b) Yamada, T.; Fukuhara, G.; Kaneda, T. *Chem. Lett.* **2003**, *32*, 534. (c) Nishiyabu, R.; Kano, K. *Eur. J. Org. Chem.* **2004**, 4985.

CHART 1. Modified β-Cyclodextrin As a Photosensitizing Host 1 and Reference Sensitizer 2

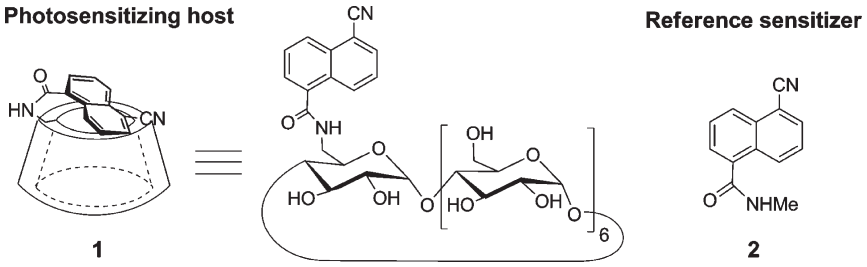

expand the scope of the entropy control concept to supramolecular photochirogenesis.

Supramolecular photochirogenesis with a built-in sensitizer is not restricted to the unimolecular reactions but is also applicable to bimolecular reactions. Thus, the enantiodifferentiating anti-Markovnikov photoaddition of methanol to 1,1-diphenylpropene (**DPP**) (Scheme 1), which was originally studied in organic solvents[18] and more recently in supercritical carbon dioxide,[19] was effected by using 6-(5-cyanonaphthyl-1-carboamido)-6-deoxy-β-cyclodextrin (**1**) as a sensitizing host (Chart 1).[12i] For such a reaction performed in aqueous methanol, it is likely that radical cationic **DPP** formed upon photoelectron transfer to the sensitizing host is attacked not only by methanol but also by water, but we could not definitely identify the water adduct under the gas chromatographic conditions established for analyzing the methanol adduct, probably due to the dehydration of the water adduct.

SCHEME 1. Enantiodifferentiating Anti-Markovnikov Photoaddition of Water and Methanol to 1,1-Diphenylpropene (DPP) in the Presence of Sensitizing Host 6-(5-Cyanonaphthyl-1-carboamido)-6-deoxy-β-cyclodextrin (1)

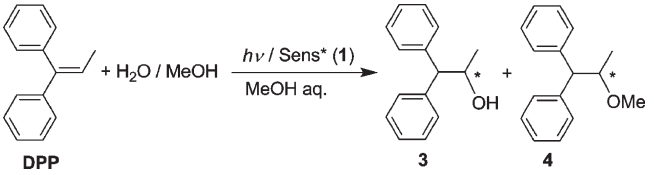

In the present study, we wanted to fully elucidate the factors and mechanisms operating in the supramolecular complexation and the competitive photochirogenic nucleophilic attack of water and methanol to **DPP** sensitized by cyanonaphthalene-modified β-cyclodextrin **1**, as well as the role of entropy in this bimolecular supramolecular photochirogenic reaction. Thus, the following aspects will be discussed in detail: (1) the self-inclusion behavior of the sensitizing moiety in host **1** and the complexation of **DPP** by host **1** in the ground state, (2) the competitive enantiodifferentiating anti-Markovnikov photoaddition of water and methanol to **DPP** included and sensitized by **1**, with a particular emphasis on water adduct **3** which was examined for the first time, and (3) the temperature and solvent effects on the yield and ee of both adducts and the roles of entropy upon supramolecular complexation and photochirogenesis.

Results and Discussion

Self-Inclusion Behavior of Host 1. Circular Dichroism Spectral Examinations. Modified cyclodextrins possessing a hydrophobic substituent are known to intramolecularly include the appended substituent moiety to give self-inclusion complexes[20] or intermolecularly assemble to form supramolecular polymers[21] particularly at high concentrations

(18) (a) Asaoka, S.; Kitazawa, T.; Wada, T.; Inoue, Y. *J. Am. Chem. Soc.* **1999**, *121*, 8486. (b) Asaoka, S.; Wada, T.; Inoue, Y. *J. Am. Chem. Soc.* **2003**, *125*, 3008.

(19) (a) Nishiyama, Y.; Kaneda, M.; Saito, R.; Mori, T.; Wada, T.; Inoue, Y. *J. Am. Chem. Soc.* **2004**, *126*, 6568. (b) Nishiyama, Y.; Kaneda, M.; Asaoka, S.; Saito, R.; Mori, T.; Wada, T.; Inoue, Y. *J. Phys. Chem. A* **2007**, *121*, 13432. (c) Nishiyama, Y.; Wada, T.; Mori, T.; Inoue, Y. *Chem. Lett.* **2007**, *36*, 1488. (d) Nishiyama, Y.; Wada, T.; Asaoka, S.; Mori, T.; McCarty, T. A.; Kraut, N. D.; Bright, F. V.; Inoue, Y. *J. Am. Chem. Soc.* **2008**, *130*, 7526.

(20) For examples: (a) Ueno, A.; Tomita, Y.; Osa, T. *Tetrahedron Lett.* **1983**, *24*, 5245. (b) Ueno, A.; Moriwaki, F.; Osa, T.; Hamada, F.; Murai, K. *J. Am. Chem. Soc.* **1988**, *110*, 4323. (c) Ueno, A.; Suzuki, I.; Osa, T. *J. Am. Chem. Soc.* **1989**, *111*, 6391. (d) Ueno, A.; Fukushima, M.; Osa, T. *J. Chem. Soc., Perkin Trans. 2* **1990**, 1067. (e) Fukushima, M.; Osa, T.; Ueno, A. *J. Chem. Soc., Chem. Commun.* **1991**, 15. (f) Ueno, A.; Kuwabara, A.; Nakamura, A.; Toda, F. *Nature* **1992**, *356*, 136. (g) Hamasaki, K.; Ikeda, H.; Nakamura, A.; Ueno, A.; Toda, F.; Suzuki, I.; Osa, T. *J. Am. Chem. Soc.* **1993**, *115*, 5035. (h) Kuwabara, T.; Nakamura, A.; Ueno, A.; Toda, F. *J. Phys. Chem.* **1994**, *98*, 6297. (i) Kuwabara, T.; Nakamura, A.; Ueno, A.; Toda, F. *J. Chem. Soc., Chem. Commun.* **1994**, 689. (j) Corradini, R.; Dossena, A.; Marchelli, R.; Panagia, A.; Sartor, G.; Saviano, M.; Lombardi, A.; Pavone, V. *Chem.—Eur. J.* **1996**, *2*, 373. (k) Ikeda, H.; Nakamura, M.; Ise, N.; Oguma, N.; Nakamura, A.; Ikeda, T.; Toda, F.; Ueno, A. *J. Am. Chem. Soc.* **1996**, *118*, 10980. (l) Corradini, R.; Dossena, A.; Galaverna, G.; Marchelli, R.; Panagia, A.; Sartor, G. *J. Org. Chem.* **1997**, *62*, 6283. (m) Matsushita, A.; Kuwabara, T.; Nakamura, A.; Ikeda, H.; Ueno, A. *J. Chem. Soc., Perkin Trans. 2* **1997**, 1705. (n) Kuwabara, T.; Takamura, M.; Matsushita, A.; Ikeda, H.; Nakamura, A.; Ueno, A.; Toda, F. *J. Org. Chem.* **1998**, *63*, 8729. (o) Ueno, A.; Ikeda, A.; Ikeda, H.; Ikeda, T.; Toda, F. *J. Org. Chem.* **1999**, *64*, 382. (p) Tanabe, T.; Usuji, S.; Nakamura, A.; Ueno, A. *J. Inclusion Phenom. Macrocyclic Chem.* **2000**, *36*, 79. (q) Kuwabara, T.; Aoyagi, T.; Takamura, M.; Matsushita, A.; Nakamura, A.; Ueno, A. *J. Org. Chem.* **2002**, *67*, 720. (r) Fukuhara, G.; Fujimoto, T.; Kaneda, T. *Chem. Lett.* **2003**, *32*, 536. (s) Miyauchi, M.; Harada, A. *J. Am. Chem. Soc.* **2004**, *126*, 11418. (t) Wang, H.; Cao, R.; Ke, C.-F.; Liu, Y.; Wada, T.; Inoue, Y. *J. Org. Chem.* **2005**, *70*, 8703. (u) Inoue, Y.; Miyauchi, M.; Nakajima, H.; Takashima, Y.; Yamaguchi, H.; Harada, A. *Macromolecules* **2007**, *40*, 3256. This paper is a mixture of intra- and intermolecular complexes: (v) Inoue, Y.; Kuad, P.; Okumura, Y.; Takashima, Y.; Yamaguchi, H.; Harada, A. *J. Am. Chem. Soc.* **2007**, *129*, 6396.

(21) For examples, see: (a) Petter, R. C.; Salek, J. S.; Sikorski, C. T.; Kumaravel, G.; Lin, F.-T. *J. Am. Chem. Soc.* **1990**, *112*, 3860. (b) Tong, L.-H.; Hou, Z.-J.; Inoue, Y.; Tai, A. *J. Chem. Soc., Perkin Trans. 2* **1992**, 1253. (c) McAlpine, S. R.; Garcia-Garibay, M. A. *J. Am. Chem. Soc.* **1998**, *120*, 4269. (d) Bügler, J.; Sommerdijk, N. A. J. M.; Visser, A. J. W. G.; van Hoek, A.; Nolte, R. J. M.; Engbersen, J. F. J.; Reinhoudt, D. N. *J. Am. Chem. Soc.* **1999**, *121*, 28. (e) Mirzoian, A.; Kaifer, A. E. *Chem. Commun.* **1999**, 1603. (f) Fujimoto, T.; Sakata, Y.; Kaneda, T. *Chem. Commun.* **2000**, 2143. (g) Hoshino, T.; Miyauchi, M.; Kawaguchi, Y.; Yamaguchi, H.; Harada, A. *J. Am. Chem. Soc.* **2000**, *122*, 9876. (h) Liu, Y.; You, C.-C.; Zhang, M.; Weng, L.-H.; Wada, T.; Inoue, Y. *Org. Lett.* **2000**, *2*, 2761. (i) Onagi, H.; Easton, C. J.; Lincoln, S. F. *Org. Lett.* **2001**, *3*, 1041. (j) Stanier, C. A.; Alderman, S. J.; Claridge, T. D. W.; Anderson, H. L. *Angew. Chem., Int. Ed.* **2002**, *41*, 1769. (k) Park, J. W.; Song, H. E.; Lee, S. Y. *J. Org. Chem.* **2003**, *68*, 7071. (l) Liu, Y.; Fan, Z.; Zhang, H.-Y.; Diao, C.-H. *Org. Lett.* **2003**, *5*, 251. (m) Liu, Y.; Fan, Z.; Zhang, H.-Y.; Yang, Y.-W.; Ding, F.; Liu, S.-X.; Wu, X.; Wada, T.; Inoue, Y. *J. Org. Chem.* **2003**, *68*, 8345. (n) Miyauchi, M.; Takashima, Y.; Yamaguchi, H.; Harada, A. *J. Am. Chem. Soc.* **2005**, *127*, 2984. (o) Harada, A.; Takashima, Y.; Yamaguchi, H. *Chem. Soc. Rev.* **2009**, *38*, 875 and references therein .

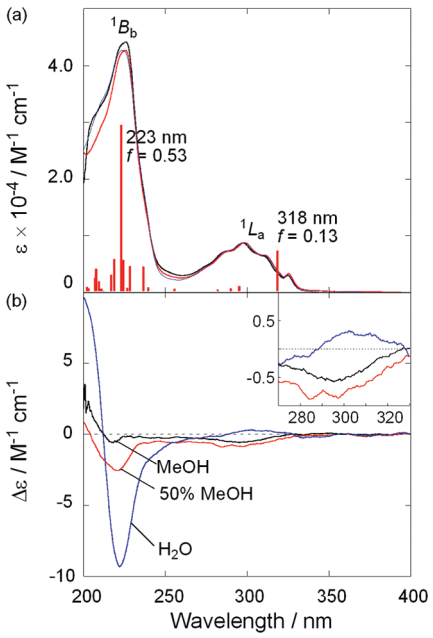

FIGURE 1. (a) UV−vis and (b) CD spectra of a 1.45×10^{-5} M solution in pure methanol (black line), a 1.52×10^{-5} M solution in 50% aqueous methanol (red line) and a 1.37×10^{-5} M solution in pure water (blue line) of **1** at 25 °C. The red bars indicate the oscillator strengths calculated by the TD-DFT calculations, and the inset shows the magnified CD spectra in the ^1L_a band region.

in aqueous solutions and in the solid state. Hence, the self-inclusion behavior of host **1** was first investigated before examining the complexation of **DPP** added as a guest substrate.

Circular dichroism (CD) spectroscopy is a powerful and indispensable tool[22] for elucidating the position and orientation of an achiral chromophoric guest included in the cyclodextrin cavity from the signs of the induced circular dichroism (ICD) signals at the chromophore's absorption bands, as proposed by Kajtar et al.,[23a] Harata et al.,[23b] and Kodaka et al.[23c]

UV−vis and CD spectra of **1** were measured in aqueous solutions of varying methanol contents. As shown in Figure 1, the ^1B_b band at ca. 225 nm displayed a negative ICD signal, intensity of which was dramatically decreased with increasing methanol content from 0 to 100%, indicating less efficient self-inclusion of the naphthalene moiety in highly methanolic solutions. Interestingly, the ^1L_a band centered at ca. 300 nm switched the sign of ICD from positive to negative by increasing the methanol content, while keeping the UV original spectral shape and intensity. To apply the sector rules[23] to the observed ICD signals, the directions of the transition moments of the naphthalene choromophore of **1** have to be determined, and hence we carried out the TD-DFT calculations on reference compound **2**, which contains the essential chromophore of **1**.

CHART 2. Directions of the ^1B_b and ^1L_a Transition Moments of 2 Calculated by TD-DFT Calculations

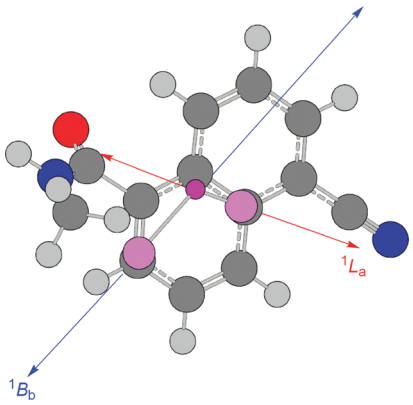

The TD-DFT calculations were performed with the B3LYP functional[24] and the aug-cc-pVDZ basis set[25] to give a major band at 223 nm with an oscillator strength of 0.53, which is assigned to the ^1B_b transition, and a minor band at 318 nm with an oscillator strength of 0.13 assignable to the ^1L_a transition, both of which nicely agree in energy and relative intensity with the experimental spectra,[26] as shown in Figure 1a. This allowed us to determine the directions of the ^1B_b and ^1L_a transition moments of **2**, as illustrated in Chart 2, and also the orientation of the appended naphthalene moiety in the cyclodextrin cavity by using the sector rules.[23] In pure or aqueous methanol, both of the ^1B_b and ^1L_a bands show negative Cotton effects, indicating that these two transition moments lay in the negative region outside of the sector cone and hence the naphthalene moiety of **1** is deduced to rest laterally on the cyclodextrin rim, as schematically drawn in Figure 2a. In water, the ^1L_a band switches the ICD sign to positive, while the ^1B_b band signal is significantly enhanced in intensity keeping the ICD sign negative, which indicates the tilted conformation shown in Figure 2b. This conformational change is likely to be caused by the increased solvent

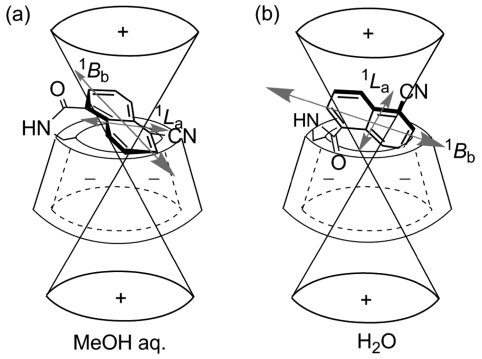

FIGURE 2. Schematic drawing of the sector rule[23a] applied to host **1** in (a) aqueous methanol and (b) water.

(22) (a) Harada, N.; Nakanishi, K. In *Circular Dichronic Spectroscpy-Exciton Coupling in Organic Sterochemistry*; University Science Books: Mill Valley, CA, 1983. (b) Berova, N.; Nakanishi, K. In *Circular Dichroism: Principles and Applications*, 2nd ed.; Berova, N., Nakanishi, K., Woody, R. W., Eds.; Wiley: New York, 2000; pp 337−382. (c) Berova, N.; Bari, L. D.; Pescitelli, G. *Chem. Soc. Rev.* **2007**, *36*, 914.

(23) (a) Kajtar, M.; Horvath-Toro, C.; Kuthi, E.; Szejtli, J. *Acta Chim. Acad. Sci. Hung.* **1982**, *110*, 327. (b) Harata, K.; Uedaira, H. *Bull. Chem. Soc. Jpn.* **1975**, *48*, 375. (c) Kodaka, M. *J. Am. Chem. Soc.* **1993**, *115*, 3702.

(24) (a) Petersson, G. A.; Bennett, A.; Tensfeldt, T. G.; Al-Laham, M. A.; Shirley, W. A.; Mantzaris, J. *J. Chem. Phys.* **1988**, *89*, 2193. (b) Stephens, P. J.; Devlin, F. J.; Chabalowski, C. F.; Frisch, M. J. *J. Phys. Chem.* **1994**, *98*, 11623. (c) Stephens, P. J.; Devlin, F. J.; Ashwar, C. S.; Chabalowski, C. F.; Frisch, M. J. *Faraday Discuss., Chem. Soc.* **1994**, *99*, 103.

(25) Dunning, T. H. *J. Chem. Phys.* **1989**, *90*, 1007.

(26) Judging from the consistent CD spectra of **1** at 10 μM to 1 mM concentrations in 25% aqueous methanol at 25 °C (Figure S2 in Supporting Information), we can rule out the formation of supramolecular aggregates at least under the conditions employed.

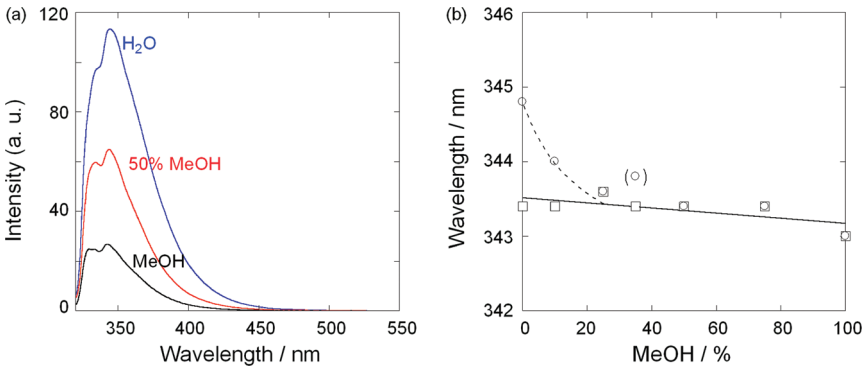

FIGURE 3. (a) Fluorescence spectra of **1** excited at 300 nm in water, 50% methanol, and methanol at room temperature; [**1**] = 1.0×10^{-5} M and (b) the fluorescence maxima of **1** (○) and **2** (□), both at 1.0×10^{-5} M concentration, as a function of methanol content.

polarity to more efficiently accommodate the hydrophobic part of naphthalene in the cavity and simultaneously expose the polar cyano group to bulk water. This result shows that the naphthalene chromophore suffers a dynamic conformational change from the capping to slant orientation by simply increasing the solvent polarity.

Fluorescence Spectral Examinations. Naphthalene derivatives are highly fluorescent in general, and can be used as a probe for sensing the environmental changes upon inclusion complexation with cyclodextrin. In the present case, the appended cyanonaphthalene moiety of **1** functions as a built-in fluorescence probe. As shown in Figure 3a, the fluorescent intensity of **1** was significantly enhanced by increasing the water content in methanol. However, reference compound **2** also exhibited a similar fluorescence intensity enhancement to a slightly larger extent (Figure S3 in the Supporting Information), and therefore the fluorescence intensity does not appear to be suitable for examining the self-inclusion behavior of the naphthalene moiety. In contrast to the fluorescent intensity which is very sensitive to the solvent polarity, the fluorescence maximum of **2**, that is, the 0−1 band, stayed constant at 343.0−343.5 nm over the entire solvent composition from pure methanol to pure water, as shown in Figure 3b. Interestingly, the fluorescence maximum of **1** showed appreciable bathochromic shifts only in the aqueous solutions containing <25% methanol, suggesting the inclusion of the naphthalene chromophore in the hydrophobic cavity of **1** with accompanying conformational changes, which is consistent with the conclusion derived from the CD spectral examinations.

NMR Spectral Examination. A series of sophisticated 2D-NMR techniques have been developed for the use in detailed conformational analysis of modified cyclodextrins.[27] In the present study, we assigned all of the protons in **1** with the aid of 2D-COSY, TOCSY, ROESY, HMBC and HMQC techniques.[20g] The assignments are summarized in Figure 4; see Chart 3 for the notation and numbering.

The chemical shifts of H1−H6 protons of each pyranose unit (A−G) in **1** are deviated to different extent from the original positions observed in native β-cyclodextrin. The deviation in chemical shift is a direct measure of the anisotropy of the naphthalene's ring current, and therefore the degree of deviation, summarized for H1−H6 of each

CHART 3. Notation of Pyranose Units and Numbering of Protons of 1

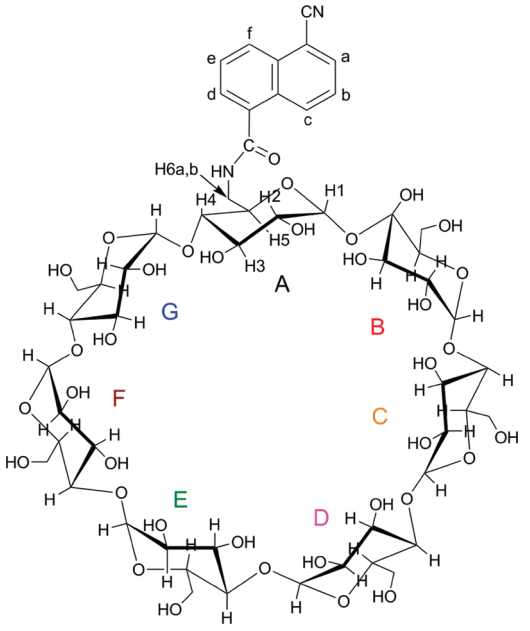

pyranose in Figure 5, is indispensable in assigning the location and orientation of the appended naphthalene in the cyclodextrin cavity. The H3 protons, located inside the cavity near the secondary rim, do not show any appreciable deviation and only the H5 and H6 protons, located near the primary rim, suffer substantial changes in chemical shift, indicating that the naphthalene is shallowly included in the cavity and no supramolecular aggregation occurs even at this concentration. Thus, only the H5 and H6a protons of pyranose A and the H5 and H6a,b protons of pyranose G deviate to the down fields, while the H5 and H6 protons of pyranoses B−E and the H6b of pyranose A show moderate to large upfield shifts. These chemical shift changes are fully compatible with the shallow inclusion of tilted naphthalene deduced from the CD spectral examinations, and further indicate that the naphthalene moiety inserts into the cavity in between the pyranose A and G, causing the downfield shifts of their H5 protons, and leans over the pyranose E-G, causing the up-fields shifts of their H5 and H6 protons. The contrasting behavior of two H6 protons of pyranose A and the large upfield shift of the H6b of pyranose B support

(27) Schneider, H.-J.; Hacket, F.; Rüdiger, V.; Ikeda, H. *Chem. Rev.* **1998**, *98*, 1755 and references therein .

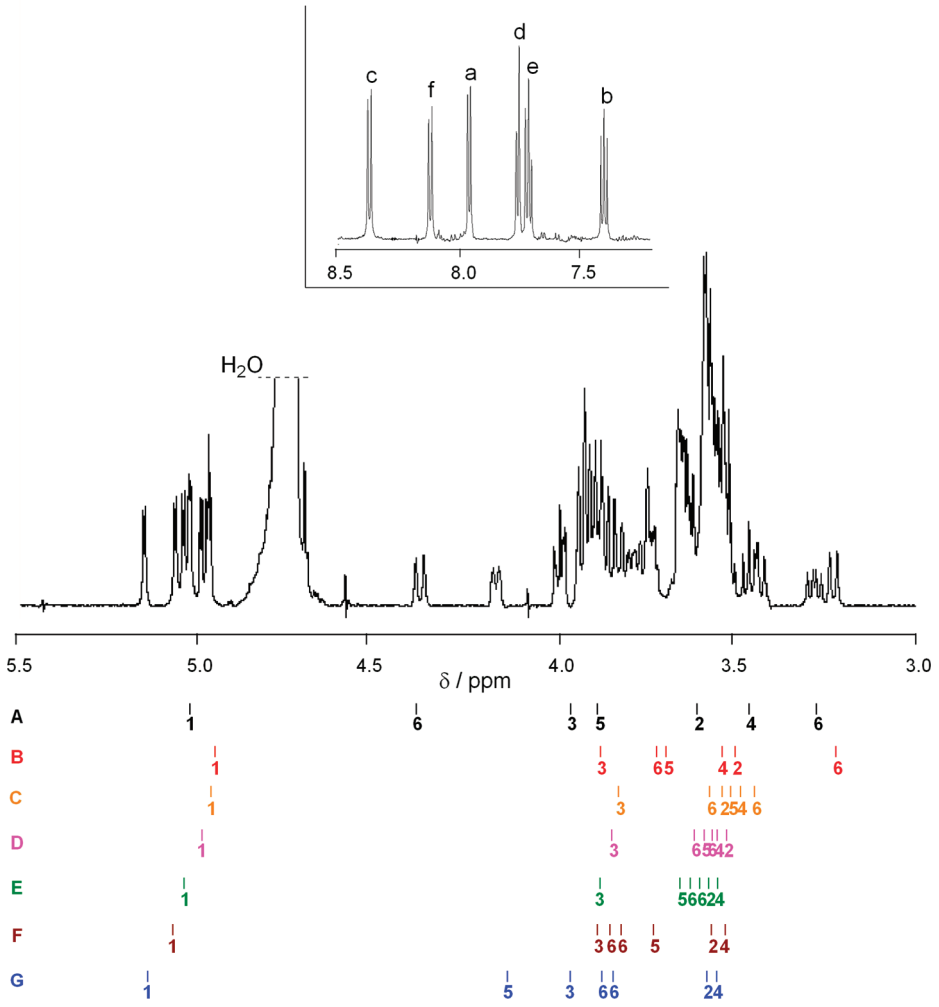

FIGURE 4. Aromatic (top) and sugar (middle) region of the 600 MHz ^{1}H NMR spectrum of a 19.2 mM solution of **1** in D_2O at room temperature; see Chart 3 for the notation of the pyranose units and the numbering of the protons.

the above assignment that the naphthalene moiety is tilted to the pyranose G side.

ROESY spectral study more clearly revealed the location and orientation of the appended naphthalene moiety in the cyclodextrin cavity. As shown in Figure 6, the naphthalene's a, b, and d protons are correlated with the H5 protons of pyranose E, D and B, respectively. These results indicate that the naphthalene moiety is shallowly included and tilts to some extent to the E−G rings. The strong NOE cross peaks of the naphthalene's c proton with the H6 of pyranose G and of the d proton with the H6 of pyranose C further support the above assignment.

Complexation of DPP with Host 1. The complexation behavior of **DPP** with **1** was first examined by UV−vis and CD spectral titrations. As shown in Figure 7a, gradual addition of **DPP** to a 0.128 mM solution of **1** in 3:1 (v/v) water−methanol did not cause any appreciable change in the naphthalene absorption but simply increased the absorbance at shorter wavelengths, which is assignable to the absorption of **DPP**. However, the addition of **DPP** induced significant changes in CD spectrum (Figure 7b), that is, the reduction of intensity in the naphthalene's ^1L_a region and the significant enhancement in the **DPP**'s ^1L_b region, with accompanying

SCHEME 2. Complexation of DPP by Host 1

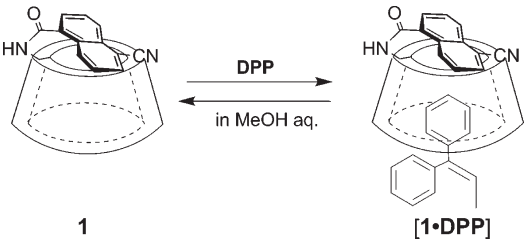

isodichroic point. As illustrated in Figure 7d, the CD intensity at 260 nm increased almost linearly with increasing **DPP** concentration, but suddenly leveled off at the stoichiometric concentration, most probably due to the precipitation of uncomplexed **DPP** at the higher concentrations, as indicated by the UV absorbance plot (Figure 7c).[28] This observation indirectly indicates the formation of 1:1 complex of **DPP** with **1** as illustrated in Scheme 2.

(28) Upon addition of **DPP** into D_2O solution of **1**, the white solid that would be supramolecular complex consisting of **1** and **DPP** precipitated under NMR condition.

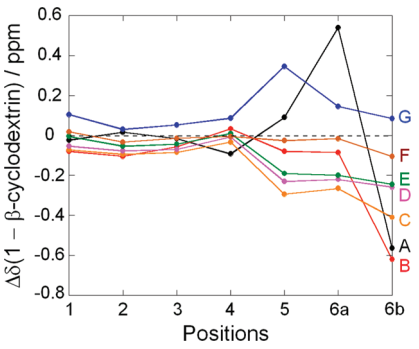

FIGURE 5. Deviation in chemical shift ($\Delta\delta$) of the H1−H6 protons of pyranose units A−G in **1** from those of native β-cyclodextrin.

The complexation behavior of host **1** with **DPP** was further investigated in aqueous methanol of different compositions by examining the CD spectral changes upon addition of **DPP**. As shown in Figure 8a, the original CD spectrum of **1** (1 mM) was not appreciably affected by the addition of an equimolar amount of **DPP** in pure methanol, indicating no interaction with **1** in the organic solvent. However, the addition of an equimolar amount of **DPP** to a less-concentrated 0.1 mM solution of **1** caused noticeable changes in CD spectrum in 50% aqueous methanol and particularly in pure water. The negative Cotton effect induced in the **DPP**-absorbing region, clearly shown in the difference CD spectra (Figure 8b), indicates the inclusion complexation of **DPP** by host **1** in the aqueous solutions. It is interesting that, despite the difference in the original orientation of the naphthalene moiety, the ICD signals observed in 50% methanol and pure water, share the same sign, indicating similar penetration mode upon inclusion complexation of **DPP** by **1**. Unfortunately, the absolute CD spectral changes were not sufficiently large ($\Delta\Delta\varepsilon < 1\ M^{-1}\ cm^{-1}$) for accurately determining the binding constant even in pure water.

Steady-state fluorescence spectral and fluorescence lifetime studies were performed to elucidate the excited-state supramolecular interactions of **DPP** with host **1**. Figure 9 shows the fluorescence spectra of **1** (1.0×10^{-5} M) in the presence and absence of an equimolar amount of **DPP** in pure methanol, 50% aqueous methanol, and pure water. In pure methanol, the fluorescence spectrum of **1** was not affected at all by the addition of **DPP**, which is reasonable as **DPP** does not form any complex with **1** in methanol (see the CD Spectral Examination) and is too dilute to dynamically quench the fluorescence of **1**. In 50% methanol, the shape of the fluorescence spectrum in the presence of **DPP** was slightly different in particular at longer wavelengths. However, in pure water, where the complexation of **DPP** with **1** is highly encouraged, the fluorescence of **1** was clearly quenched by **DPP** included in the cavity. More detailed analysis of the fluorescence quenching behavior in 50% methanol and in water will be discussed later.

The fluorescence lifetimes of **1** in the presence and absence of **DPP** were measured in water−methanol mixed solvents of varying compositions by means of the time-correlated single-photon-counting technique. The results obtained are summarized in Table 1. The naphthyl fluorophore in **1** showed an apparently single-exponential decay in aqueous solutions containing 0−50% methanol, which is somewhat

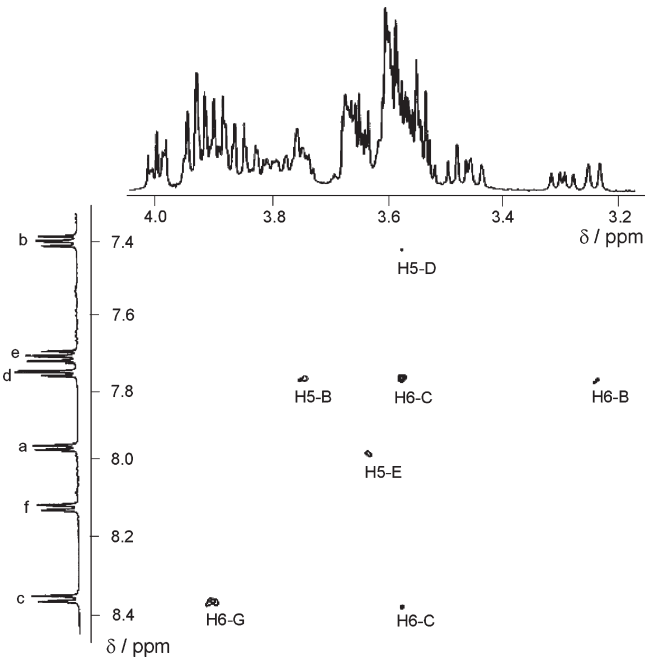

FIGURE 6. Partial ROESY spectrum of **1** in D_2O obtained with a mixing time of 1.5 s and the assignment of the cross peaks.

different from the previous observations that a fluorophore appended to cyclodextrin generally gives two lifetimes attributable to free and included species.[20j−l,o] The present observation may be ascribed to the total inclusion of the naphthyl moiety as a result of its highly hydrophobic nature or to the comparable lifetimes for both species as a result of the shallow inclusion. The inherent lifetime of **1** gradually increased with increasing water content, as was the case with the fluoresce intensity (Figure 9). In the presence of **DPP**, the lifetime was not apparently changed (within the instrumental error of ± 0.1 ns) at higher methanol contents, but was appreciably shortened due to the quenching by **DPP** in solutions of high water content. These results indicate that in high water-content solutions the naphthyl moiety is totally self-included in the cyclodextrin cavity and its fluorescence is quenched even by 10 μM **DPP** without accompanying appreciable exciplex fluorescence.

Competitive Photoaddition of Water and Methanol to DPP Included and Sensitized by Host 1. The enantiodifferentiating anti-Markovnikov photoaddition of water and methanol to **DPP** (Scheme 3) was mediated by sensitizing host **1** in aqueous methanol at different temperatures to give chiral water adduct **3** and methanol adduct **4** in varying yields and ee's. As shown in Table 2,[29] no adduct was produced in pure methanol upon irradiation of 0.1 mM **DPP** with 1 mM **1**. This seems reasonable since the affinity of **DPP** to host **1** is extremely low in methanol in particular at the concentrations employed, as demonstrated by the lack of ICD (Figure 8b) and the negligible fluorescence spectral change (Figure 9) upon addition of **DPP** to a methanol solution of **1**. By increasing the **DPP** concentration up to 20 mM and extending the irradiation period to 16 h, a trace amount of methanol adduct **4** was detected by GC but the ee was only 1.7% at

(29) The method of supramolecular photosensitizations of **DPP** included by **1** was shown in the Experimental Section.

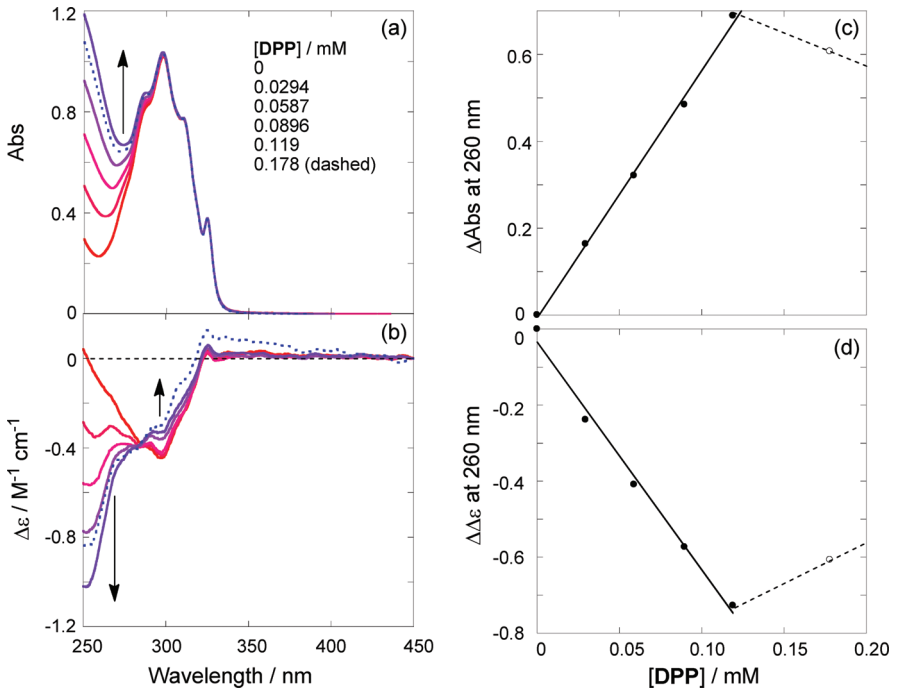

FIGURE 7. (a) UV−vis and (b) CD spectra of 3:1 (v/v) H_2O-MeOH solutions of **1** (0.128 mM; fixed) and **DPP** (0−0.178 mM) at 25 °C and (c) the absorbance and (d) circular dichroism changes at 260 nm as functions of the **DPP** concentration.

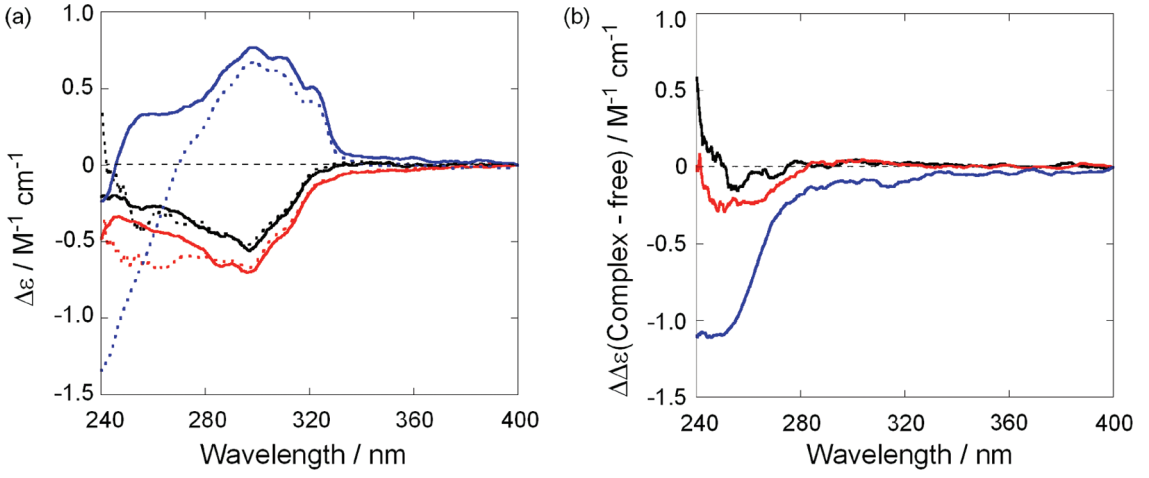

FIGURE 8. (a) CD spectra of **1** in the absence (solid line) and presence (dashed line) of **DPP** at 25 °C; Black, [**1**] = [**DPP**] = 1.0 mM in pure methanol (1 mm cell); Red, [**1**] = [**DPP**] = 0.1 mM in 50% aqueous methanol (1 cm cell); Blue, [**1**] = [**DPP**] = 0.1 mM in pure water (1 cm cell). (b) Corresponding CD spectral changes ($\Delta\Delta\varepsilon$: difference in circular dichroism) caused by the addition of **DPP** to **1**.

25 °C and −2.8% at −40 °C.[30] This indicates that **DPP** is not included in the cavity and hence the photoreaction occurs in bulk methanol, where the cyclodextrin simply functions as a chiral auxiliary attached to the naphthalene sensitizer, as was the case in the conventional asymmetric photosensitization in organic solutions.[5−8,18] However, the addition of ≥25% water to methanol greatly accelerated the photoreaction even in a dilute solution containing 0.1 mM each of **DPP** and **1**, as shown in Table 2. Thus, 71−99% of **DPP** was consumed after 2 h irradiation in aqueous methanol to give water adduct **3** and methanol adduct **4** in 25−74% combined yields, along with a varying amount of benzophenone as an oxidation product despite the argon bubbling prior to the irradiation. Judging from the CD spectral changes of **1** upon addition of **DPP** in aqueous methanol shown in Figure 8, we may conclude that this remarkable acceleration was accomplished through the enhanced binding of **DPP** by **1** and the subsequent photoinduced electron transfer from **DPP** to the excited naphthalene moiety closely located in the cavity. Consequently, the photosensitization mechanism is switched from the conventional molecular level in pure methanol to the supramolecular regime in aqueous methanol solutions.

Effect of Conversion on Product ee. This photoaddition reaction is irreversible and the product's ee is not expected to depend on the conversion of substrate as long as the host−guest complexation is maintained until the end of the reaction. To confirm this, we performed the photoreaction of

(30) GC chromatographic condition of **4** was shown in the Supporting Information (Instruments in General Experimental Methods).

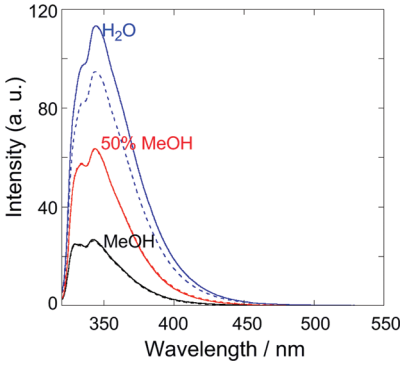

FIGURE 9. Fluorescence spectra of **1** in the absence (solid lines) and presence (dashed lines) of **DPP** at room temperature; [**1**] = [**DPP**] = 1.0×10^{-5} M, excitation wavelength was 300 nm.

TABLE 1. Fluorescence Lifetimes (τ/ns) of 1 and 2 in the Presence/Absence of DPP in Aqueous Methanol[a]

		additive	
compd	% methanol	none	**DPP**[b]
1	50	0.6	0.6
	35	0.8	0.8
	25	1.0	0.8
	10	1.0	0.8
	0	1.4	1.0
2	25	0.7	[c]

[a]Measured with 1.0×10^{-5} M solutions of **1** and **2** at room temperature under aerated (nondegassed) conditions by the time-correlated single-photon-counting technique; error ± 0.1 ns. [b][**DPP**] = 1.0×10^{-5} M. [c]Not determined.

DPP mediated by **1** for varying periods of irradiation (from 5 min to 2 h) in 25% methanol solution at −10 °C (a condition that guarantees strong complexation), and the conversion and the ee of methanol adduct **4** were determined. As shown in Table 2, the ee of **4** obtained for different irradiation periods nicely agreed with each other to give an average value of 10.6 ± 0.7%, indicating that we can safely discuss the product's ee obtained at any irradiation period or conversion at least for those obtained in high water-content solutions at low temperatures.

Effects of Solvent Composition and Temperature on Product Ratio 3/4. In this competitive photoaddition of water and methanol to **DPP**, the product ratio **3**/**4** is a critical function of the solvent composition, as can be seen from Table 2. However, by taking into account of the molar ratio of the attacking agents, i.e. water and methanol, the relative reactivity for water versus methanol was calculated as shown in Table 3. The relative reactivity thus obtained at 45, 25, or −10 °C is constant, irrespective of the water/methanol ratio. Interestingly, the temperature effect on the relative reactivity is modest and somewhat puzzling, displaying an appreciable increase from 0.35 to 0.45 by decreasing the temperature from 45 to −20 °C but a subsequent decrease to 0.34 at −45 °C. By assuming that the temperature does not greatly affect the relative reactivity, we obtain an overall average of 0.40 ± 0.06 for the competitive photoaddition of water and methanol to **DPP**. This value indicates that the attack of water to radical cationic **DPP**, which is produced upon photoinduced electron transfer to the naphthyl moiety of **1** within the cyclodextrin cavity, is slower or less efficient by a factor of 2.5 than that of methanol. This seems reasonable

SCHEME 3. Enantiodifferentiating Anti-Markovnikov Photoaddition of Water and Methanol to DPP Included and Sensitized by 1

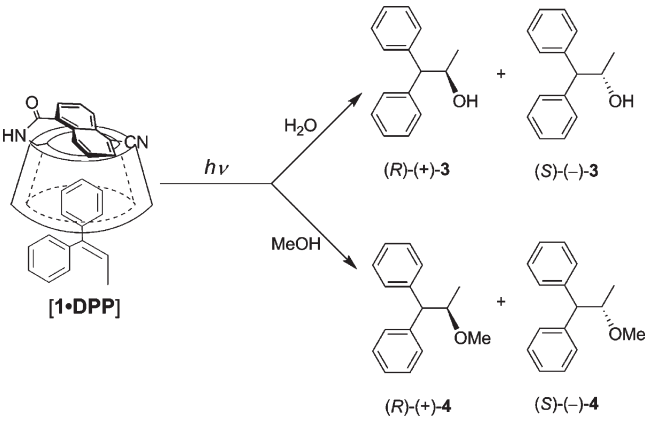

in view of the nucleophilic nature of the water/methanol attack to **DPP** and the higher acidity, or lower basicity, of water (pK_a = 14.0 at 25 °C)[31] than that of methanol (pK_a = 15.5 at 25 °C).[31]

Enantiodifferentiation Mechanisms. There are two potentially enantiodifferentiating steps in this supramolecular photochirogenic reaction, which are the complexation of **DPP** by host **1** in the ground state and the subsequent photoaddition of water/methanol in the excited state. In principle, both of the thermodynamic and kinetic processes contribute to the discrimination of the enantiofaces of **DPP**. As illustrated in Scheme 4, the two enantiofaces of the olefinic part of **DPP** are differentiated upon complexation with chiral host **1** to give a pair of diastereomeric complexes (with equilibrium constants K_r and K_s). In these complexes, either *re*- or *si*-enantioface of **DPP** is more exposed to the bulk solution and hence attacked by water/methanol upon photoinduced electron transfer to yield (*R*)- or (*S*)-**3** or **4** at rate constant k_{rR} or k_{sS}, although the hindered face may be attacked less efficiently to give antipodal (*S*)- or (*R*)-**3** or **4** at k_{rS} or k_{sR}. Thus, the enantiomer ratio of **3** or **4** can be defined by eq 1.

$$[R]/[S] = (K_r/K_s)(k_{rR} + k_{sR})/(k_{sS} + k_{rS}) \quad (1)$$

By neglecting the minor paths (the attack from the hindered side), eq 1 is simplified to eq 2.

$$[R]/[S] = (K_r/K_s)(k_{rR}/k_{sS}) \quad (2)$$

This equation clearly indicates that the product's ee is controlled *thermodynamically* by the stability difference between the diastereomeric *re*- and *si*-complexes in the ground state and also *kinetically* by the difference in rate constant of the subsequent water or methanol attack to the radical cationic **DPP**.

Enantioselectivity and the Eyring Analysis. As discussed above, the enantioface of **DPP** can be discriminated upon (1) complexation with chiral host **1** and/or (2) the subsequent nucleophilic attack of water/methanol to radical cationic **DPP** within the chiral host cavity. If only the first step is enantioface selective and the second is *racemic* (nonenantioface-selective), the water and methanol adducts should give exactly the same ee.

(31) David. R. L. *CRC Handbook of Chemistry and Physics*; CRC Press: Boca Raton, FL, 2003−2004.

TABLE 2. Enantiodifferentiating Anti-Markovnikov Photoaddition of Water and Methanol to DPP Sensitized by Host 1 in Aqueous Methanol[a]

						yield/%[d]			ee/%	
% MeOH ([H_2O]/[MeOH][b])	[**DPP**]/mM	[**1**]/mM	temperature/°C	irradiation time/h	conversion/%[c]	**3**[e]	**4**[f]	**3/4**	**3**[g]	**4**[h]
100 (0)	0.1	1.0	25	2	[i]					
	20	1.0	25	16[j]	<1		[k]			1.7
			−10	16[j]	<1		[k]			−0.9
			−40	16[j]	<1		[k]			−2.8
75 (0.75)	0.1	0.1	45	2	[l]	[l]	[l]	0.28	−0.9	[l]
			25	2	71	6	19	0.32	−0.3	1.4
			−10	2	74	10	29	0.34	1.2	2.0
			−40	2	77	12	45	0.27	2.7	2.8
50 (2.24)	0.1	0.1	45	2	97	23	30	0.77	1.9	−2.1
			25	2	97	19	24	0.79	3.9	−0.8
			−10	2	>99	26	32	0.81	6.5	2.1
			−40	2	96	[l]	61	[l]	[l]	5.8
			−45	2	[l]	[l]	[l]	0.76	12.0	[l]
35 (4.16)	0.1	0.1	45	2	>99	24	17	1.4	3.5	4.3
			25	2	>99	28	19	1.5	6.0	4.8
			0	2	91	32	19	1.7	9.7	6.8
			−20	2	89	41	22	1.9	14.9	9.6
25 (6.73)	0.1	0.1	45	2	>99	36	15	2.4	4.6	6.5
			25	2	95	53	18	2.9	6.9	7.8
			15	2	>99	49	16	3.1	8.9	8.0
			0	2	>99	56	18	3.1	12.3	10.1
			−10	0.083	68	[l]	9	[l]	[l]	9.7
				0.5	88	[l]	13	[l]	[l]	11.4
				1	93	[l]	15	[l]	[l]	10.5
				2	94	46	15	3.1	14.9	10.9
10 (20.2)	0.1	0.1	45	2	>99	42	6	7.0	5.7	8.3
			25	2	93	63	6	10.5	9.4	8.7
			5	2	91	56	6	9.3	13.0	10.9
			−5	2	85	[l]	4	[l]	[l]	11.6
			−10	2	71	[l]	3	[l]	18.1	13.4
0 (∞)	0.1	0.1	45	2	[l]	[l]			6.4	
			25	2	[l]	[l]			9.4	
			10	2	[l]	[l]			13.9	
			0	2	[l]	[l]			15.6	

[a]Irradiated under an argon atmosphere in aqueous methanol with an ultrahigh-pressure Hg lamp (500 W) fitted with a UV-29 glass filter, unless stated otherwise. [b]Molar ratio. [c]Loss of starting material determined by GC. [d]Yield based on the conversion; error in yield <1%; despite the argon purge, benzophenone was produced as a side product in varying yields particularly at higher temperatures. [e]Chemical yield of water adduct **3** determined by HPLC. [f]Chemical yield of methanol adduct **4** determined by GC. [g]Enantiomeric excess of **3** determined by chiral HPLC; error in ee <1% (see the Supporting Information in Figure S4). [h]Enantiomeric excess of **4** determined by chiral GC; error in ee <0.5%. [i]No reaction. [j]Irradiated with a high-pressure Hg lamp (300 W) fitted with a uranium glass filter. [k]Value not determined due to low conversion. [l]Not determined.

TABLE 3. Relative Reactivity of Water versus Methanol upon Photoaddition to DPP Included and Sensitized by Host 1 in Aqueous Methanol

temperature/°C	[H_2O]/[MeOH]	product ratio **3/4**	relative reactivity H_2O/MeOH
45	0.75	0.28	0.37
	2.24	0.77	0.34
	4.16	1.4	0.34
	6.73	2.4	0.36
	20.2	7.0	0.35
		average	*0.35 ± 0.01*
25	0.75	0.32	0.43
	2.24	0.79	0.35
	4.16	1.5	0.36
	6.73	2.9	0.43
	20.2	10.5	0.52
		average	*0.42 ± 0.07*
15	6.73	3.1	0.46
0	4.16	1.7	0.41
	6.73	3.1	0.46
		average	*0.44 ± 0.03*
5	20.2	9.3	0.46
−10	0.75	0.34	0.45
	2.24	0.81	0.36
	6.73	3.1	0.46
		average	*0.43 ± 0.05*
−20	65:35 [4.16]	1.9	0.45
−40	25:75 [0.75]	0.27	0.36
−45	50:50 [2.24]	0.76	0.34
	overall average		*0.40 ± 0.06*

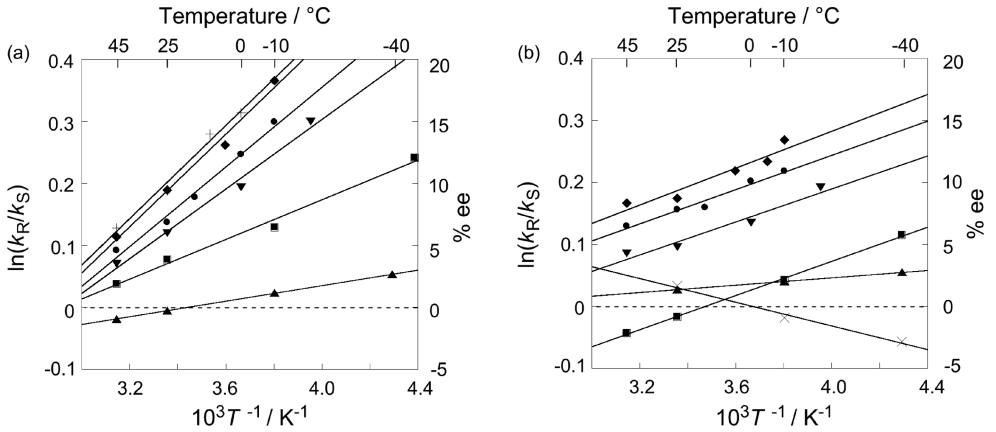

FIGURE 10. Eyring plots: Temperature dependence of the ee values of (a) water adduct **3** and (b) methanol adduct **4** obtained in the enantiodifferentiating anti-Markovnikov photoaddition of water and methanol to **DPP** included and sensitized by host **1** in methanol (×), 75% methanol (▲), 50% methanol (■), 35% methanol (▼), 25% methanol (●), 10% methanol (♦), and water (+).

SCHEME 4. Thermodynamic Enantioface Differentiation (K_r/K_s) upon Complexation of DPP with Host 1 in the Ground State and Kinetic Enantioface Differentiation (k_{rR}/k_{sS}) upon Subsequent Nucleophilic Attack of ROH (Water or Methanol) to Radical Cationic DPP Generated by Photoinduced Electron Transfer to the Cyanonaphthalene Moiety of Sensitizing Host 1[a]

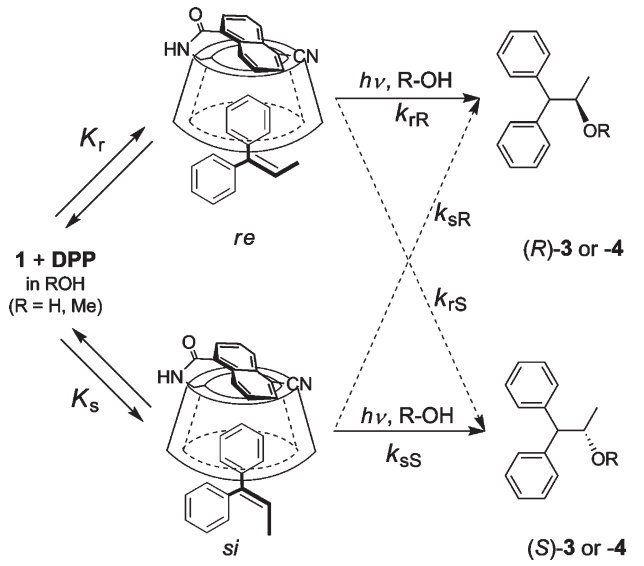

[a]"re" and "si" indicate the open enantioface (front side) in the pair of diastereomeric 1•DPP complexes, while the dotted arrow indicate the minor path involving the attack from the hindered side.

However, the experimental ee's obtained for **3** and **4** (Table 2) significantly differ from each other (by 3−5%, which exceeds the experimental error of ±1%) in several runs particularly those performed at low temperatures. This reveals that both of the complexation and the subsequent photoaddition contribute to the enantiodifferentiation. Thus, the higher ee's of 15−18% were obtained for water adduct **3** in the photoreaction performed in more hydrophilic solvents at 0 to −20 °C, while the best ee's for methanol adduct **4** (10−13% ee) were appreciably lower under the comparable conditions, probably because the faster attack of methanol is less enantioselective. The higher ee's obtained generally in more water-rich solvents at lower temperatures may be ascribed to the enhanced and tighter binding of **DPP** in host **1** cavity.

It is also interesting that the product chirality is inverted indeed or expected to be inverted within the temperature range employed. Such a remarkable phenomenon has already been reported for several conventional asymmetric photosensitizations in isotropic media[5−8,18] and also for the supramolecular enantiodifferentiating photoisomerization of (*Z*)-cyclooctene mediated by sensitizer-appended permethylcyclodextrins.[12g,k] This apparently unusual inversion of product chirality by temperature can be rationalized by using the differential Gibbs−Helmholtz equation: $\Delta\Delta G^{\ddagger} = \Delta\Delta H^{\ddagger} - T\Delta\Delta S^{\ddagger}$. At low temperatures, the differential activation free energy $\Delta\Delta G^{\ddagger}$, which determines the product's ee, is dominated by the enthalpy term $\Delta\Delta H^{\ddagger}$. However, when the signs of $\Delta\Delta H^{\ddagger}$ and $\Delta\Delta S^{\ddagger}$ are the same as in the present cases, the entropy term $T\Delta\Delta S^{\ddagger}$ overwhelms the enthalpy term $\Delta\Delta H^{\ddagger}$ at a critical (equipodal) temperature (T_0) to invert the sign of $\Delta\Delta G^{\ddagger}$ and give the antipodal product at temperatures higher than T_0.[5−8] In the present case, the differential activation parameters $\Delta\Delta H^{\ddagger}$ and $\Delta\Delta S^{\ddagger}$ obtained in the Eyring analysis are considered to be a weighted sum of the differential thermodynamic parameter for the enantioface-differentiating complexation of **DPP** with host **1** and the differential activation parameter for the enantioface-differentiating attack of water/methanol to radical cationic **DPP** within the host **1** cavity.

To quantitatively evaluate the enthalpic and entropic contributions to the enantiodifferentiation upon complexation and photoaddition, the ee data obtained at different temperatures in each aqueous methanol solution were subjected to the Eyring analysis.[5−8,18] Thus, the natural logarithm of the apparent relative rate constants for the formation of (*R*)- and (*S*)-form of **3** and **4**, that is k_R/k_S = (100 + % ee)/(100 − % ee), were plotted against the reciprocal temperature.

As illustrated in Figure 10, each set of the data points obtained for **3** in aqueous methanol of different compositions falls on a single straight line, indicating that the enantiodifferentiation mechanism does not change in the temperature range employed in each solvent. However, the data for **4** do not appear to converge at a single point as is the case for **3** in particular in solvents of high methanol contents, suggesting that the operating mechanism may not be the same upon attack of water and methanol to **DPP** in

TABLE 4. Differential Activation Parameters for Competitive Enantiodifferentiating Photoaddition of Water and Methanol to DPP Mediated by Host 1 in Aqueous Methanol Solutions at 298 K[a]

	water adduct **3**		methanol adduct **4**	
Solvent	$\Delta\Delta H^{\ddagger}_{R\text{-}S}$/kJ mol^{-1}	$\Delta\Delta S^{\ddagger}_{R\text{-}S}$/J mol^{-1} K^{-1}	$\Delta\Delta H^{\ddagger}_{R\text{-}S}$/kJ mol^{-1}	$\Delta\Delta S^{\ddagger}_{R\text{-}S}$/J mol^{-1} K^{-1}
100% MeOH			0.8	2.9
75% MeOH	−0.5	−1.8	−0.3	−0.6
50% MeOH	−1.3	−3.9	−1.2	−4.0
35% MeOH	−2.3	−6.8	−1.1	−2.9
25% MeOH	−2.7	−7.7	−1.2	−2.6
10% MeOH	−3.1	−8.8	−1.0	−1.9
H_2O	−3.1	−8.8		

[a] Error: <0.3 kJ mol^{-1} for $\Delta\Delta H^{\ddagger}$ and <1.0 J mol^{-1} K^{-1} for $\Delta\Delta S^{\ddagger}$.

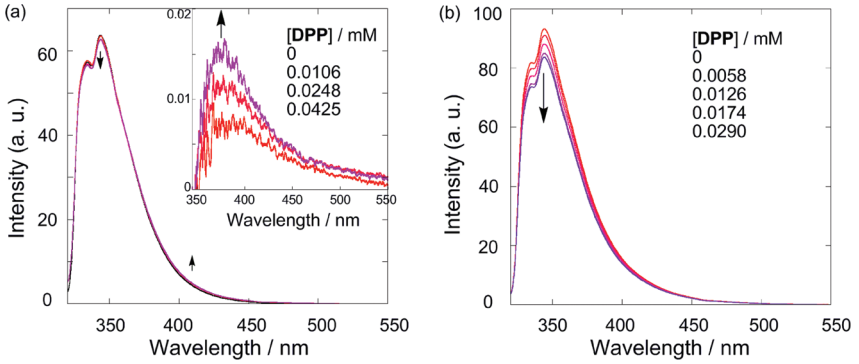

FIGURE 11. Fluorescence spectra of a 0.01 mM solution of **1** excited at 300 nm upon addition of various concentrations of **DPP** in (a) 50% MeOH and (b) 25% MeOH at room temperature. In 50% MeOH, exciplex emission obtained by spectral subtraction is shown in the inset.

highly methanolic solutions. Nevertheless, the differential activation enthalpy ($\Delta\Delta H^{\ddagger}_{R\text{-}S}$) and entropy ($\Delta\Delta S^{\ddagger}_{R\text{-}S}$) can be calculated from the slope and intercept of the Eyring plots in Figure 10; the results are listed in Table 4.

Fluorescence Quenching of 1 by DPP. To further elucidate the excited state involved in the enantiodifferentiation process and also to evaluate the rate constants of the relevant processes, we performed the fluorescence quenching experiments in aqueous solutions containing 25−50% methanol. In 50% methanol, the fluorescence of **1** was only slightly quenched by 0.0425 mM **DPP** to show a new weak emission at ca. 380 nm attributable to an exciplex intermediate (Figure 11, inset), with accompanying isoemissive point at 345 nm. In contrast, the fluorescence quenching was much more efficient in 25% methanol solution, displaying appreciable decrease of fluorescence intensity upon addition of **DPP** of up to 0.029 mM, which however did not accompany any new emission at longer wavelengths. The efficient quenching in the latter solvent may be ascribed to the enhanced binding of **DPP** by host **1**, which facilitates the subsequent static quenching within the cyclodextrin cavity.

The fluorescence quenching data obtained in 25% methanol were analyzed by using the conventional Stern−Volmer equation (eq 3) to evaluate the apparent quenching rate constant in this supramolecular complex. The relative fluorescence intensity (I_F^0/I_F) was plotted against the concentration of added **DPP** to give a good straight line up to 0.0174 mM but then level off, as shown in Figure 12. The saturation behavior may be ascribed to the full occupation of

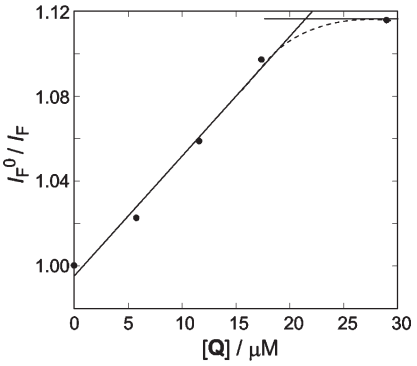

FIGURE 12. Stern−Volmer plot for fluorescence quenching of 0.01 mM **1** by **DPP** in 25% MeOH at room temperature.

host **1** cavity by **DPP**, although the binding constant could not be determined for this host−guest system for the solubility reason.[32] From the slope of the plot, the Stern−Volmer constant ($k_Q\tau^0$) was determined to be 5600 M^{-1}. The apparent quenching constant (k_Q) calculated by using the $k_Q\tau^0$ value thus obtained and the fluorescence lifetime (τ^0 = 1.0 ns, Table 1) amounts to 5.6×10^{12} M^{-1} s^{-1}. This value far exceeds the diffusion-controlled rate constants (k_{diff}) in both water (6.5×10^9 M^{-1} s^{-1})[33] and methanol (1.1×10^{10} M^{-1} s^{-1})[33] and is therefore assignable to the static quenching of the naphthyl moiety of **1** by **DPP** tightly packed in the cyclodextrin cavity, leading to the immediate electron transfer affording radical cationic **DPP**. In more

(32) As shown in the Supporting Information (Figure S5), under the diluted concentration, the binding constant was not obtained even by the fluorescence titration experiments due to the low solubility of **DPP** as revealed by UV titration.

(33) Murov. S. L. *Handbook of Photochemistry*; Marcel Dekker: New York, 1973.

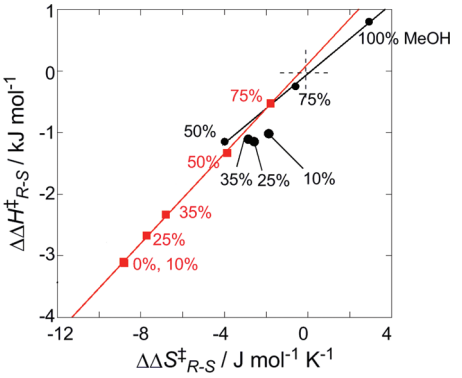

FIGURE 13. Enthalpy−entropy compensation plot of the differential activation parameters obtained for water adduct **3** (red) and methanol adduct **4** (black) in aqueous solutions of varying methanol contents from 0 to 100%.

lipophilic 50% methanol solution, it is likely that the complexation of **DPP** is much weaker and most of the **DPP** is populated in the bulk solution even at the concentration of 0.0425 mM. Furthermore, the naphthyl moiety of **1** is less tightly bound and more exposed to the bulk solution (as judged from the CD spectral changes in Figure 8), allowing the dynamic quenching by **DPP** in the bulk solution and the subsequent exciplex formation as was the case in homogeneous solution.[18]

$$I_F^0/I_F = 1+k_Q\tau^0[Q] \quad (3)$$

Enthalpy−Entropy Compensation. Compensatory enthalpy−entropy relationship has widely been observed not only for the inclusion complexation of various organic guests with cyclodextrin and other supramolecular hosts[10] but also for the enantiodifferentiating photoisomerization and photoaddition reactions sensitized by chiral aromatic compounds,[5−8] and used as a tool for globally analyzing the ground- and excited-state processes. Hence, we performed the enthalpy−entropy compensation analysis of the differential activation parameters obtained in this study for a better understanding of the enantiodifferentiating mechanism and factors operating in the photosensitized addition of water and methanol in the mixed solvents.

In Figure 13, all of the $\Delta\Delta H^{\ddagger}_{R\text{-}S}$ values listed in Table 4 are plotted against the corresponding $\Delta\Delta S^{\ddagger}_{R\text{-}S}$ values to reveal distinctly different profiles for **3** and **4**. Thus, the parameters for water adduct **3** obtained in pure water to 75% methanol gives an excellent straight line that passes through the origin, confirming that the enantiodifferentiating mechanism operating does not change throughout the methanol contents from 0 to 75%; the isokinetic temperature (T_{iso}), which is equivalent to the slope, is 365 K. In contrast, methanol adduct **4** gives a very different compensation plot with a kink (Figure 13, black line), which is related to the less regular behavior of the ee of **4** in the differential Eyring plot (Figure 10). The plot of the parameters for **4** obtained at high methanol contents (50−100%) looks normal, affording a good straight line that crosses the origin; the T_{iso} value of 283 K obtained from the slope is significantly lower than that for **3**. However, the parameters obtained for **4** in 10−35% methanol are clearly deviated from the straight line (Figure 13), probably because some different mechanism, which is not available upon the addition of water, is operating for the methanol addition in the solutions of low methanol contents. As one of such mechanisms, we may suggest the static intracavity attack of coincluded methanol[34] to **DPP** tightly bound to cyclodextrin in particular in highly hydrophobic, less methanolic solutions, which may be related to the pronounced bathochromic shift of fluorescence at low methanol contents discussed above (Figure 3). The contribution of such a mechanism, and therefore the deviation from the original compensation plot, are negligible in 50−100% methanol, but become clearer as the methanol content in aqueous solution is further reduced to 35% or less, as shown in Figure 13.

Optimization of Product ee. As shown in Table 2, the ee's of **3** and **4** are critical functions of the methanol content and the temperature, and the highest values of 18% ee for **3** and 13% for **4** were obtained upon irradiation of an equimolar mixture of **DPP** (0.1 mM) and host **1** (0.1 mM) in 10% methanol at −10 °C. This is reasonable as the major enantiodifferentiation occurs only within the chiral cavity of host **1**. In this context, it is sensible to examine the photosensitization at a much higher host concentration. Indeed, the photoreaction of **DPP** (0.1 mM) sensitized by host **1** of 2.0 mM in 10% methanol solution at −10 °C afforded water adduct **3** in an enhanced ee of 24.3% and methanol adduct **4** in a decreased ee of 8.5%. The contrasting behavior of ee observed for the water and methanol adducts is consistent with the above-mentioned mechanism. Thus, the use of a 20-fold excess amount of host enhances the complexation of **DPP**, which simply leads to a higher ee for water adduct **3** but allows the static, and therefore less enantiodifferentiating, intracavity attack of coincluded methanol to produce adduct **4** in lower ee.

We also examined the pressure effect on this enantiodifferentiating supramolecular photoaddition. However, the photosensitization of **DPP** (0.1 mM) by host **1** (2.0 mM) in 10% methanol at −19 °C under a pressure of 210 MPa gave water adduct **3** in 24.4% ee, which is comparable to that obtained above in the same solvent at −10 °C and atmospheric pressure (0.1 MPa). This means that the effects of increasing pressure and decreasing temperature are canceled to each other in this supramolecular photosensitization.

Since the temperature turned out to be an important factor to critically control the ee of **3**, we tried to decrease the freezing point of 10% methanol not by applying high pressure but by adding a salt. A 10% methanol solution of **DPP** (0.1 mM), **1** (2.0 mM), and aluminum perchlorate (1.5 M) was photolyzed at −17 °C to afford **3** in an appreciably better ee of 26.4%.

Conclusions

In the present study, we first investigated the self-inclusion behavior of host **1** and the complexation behavior of **DPP** with **1** in the ground state, and then the competitive photoaddition of water and methanol to **DPP** mediated by **1**. The supramolecular photochirogenesis mechanism turned out to involve both of the *thermodynamically controlled* enantioface-differentiating complexation of **DPP** with **1** in the ground-state equilibrium and the *kinetically controlled* enantioface-differentiating attack of water/methanol to radical cationic **DPP** within the host **1** cavity in the excited-state

(34) Huang, J.; Catena, G. C.; Bright, F. V. *Appl. Spectrosc.* **1992**, *46*, 606.

rate. However, the enthalpy−entropy compensation analysis of the differential activation parameters obtained for the supramolecular asymmetric photoaddition further revealed a difference in the mechanisms that determine the ee's of **3** and **4**, for which the static intracavity attack of coincluded methanol to **DPP** tightly included in the cyclodextrin cavity is likely to be responsible. Utilizing these mechanistic understandings, we were able to enhance the ee of water adduct **3** up to 26.4%, which is the highest value ever obtained for a bimolecular photochirogenic reaction using a chiral photosensitizing supramolecular host.

Experimental Section

Methods. The self-inclusion behavior of host **1** was investigated by UV−vis, CD, and fluorescence spectrometry in aqueous methanol solutions of different compositions at various temperatures. The self-inclusion was examined also by 2D-NMR technique. The complexation of **DPP** by host **1** was examined by the CD and fluorescence spectroscopy as well as the fluorescence lifetime measurement. Aqueous methanol solutions (2 mL) of various compositions, containing **DPP** (0.1 mM) and **1** (0.1 mM), were irradiated for 2 h under an Ar atmosphere at temperatures varying from 45 to −45 °C by using a 500-W ultrahigh-pressure mercury lamp fitted with a UV-29 glass filter, while methanol solutions (5 mL) in Pyrex tubes (1 cm i.d.), containing **DPP** (20 mM) and **1** (1.0 mM), were irradiated at >320 nm for 16 h under Ar in the same temperature range by using a 300 W high-pressure mercury lamp fitted with a uranium glass filter. The photolyzed sample, excepting for that in pure methanol, was poured onto a 10% aqueous potassium hydroxide solution (1 mL) for decomplexation. After further addition of a saturated sodium chloride solution (1 mL), the mixture was extracted with diethyl ether (1 mL). A known amount of cyclopentadecane was added to the separated organic layer as an internal standard for GC, and the ether solution was concentrated by Ar bubbling and subjected to the chiral GC analysis for determining the consumption of **DPP** and the chemical yield and ee of **4**, and also to the chiral HPLC analysis for the yield and ee of **3**. Representative HPLC chromatograms of **3** were shown in Figure S4. The photolyzed samples in pure methanol were directly injected into the GC for the analyses of **4**.

Synthesis of 2. Aqueous methylamine (40%) solution (1.0 mL, 11.6 mmol) and 5-cyanonaphthalene-1-carboxylic acid[35] (1.15 g, 5.83 mmol) were dissolved in dehydrated *N*,*N*-dimethylformamide (10 mL) in a 100 mL round-bottomed flask under an argon atmosphere. To the mixture was added 1-ethyl-3-(3′-dimethylaminopropyl)-carbodiimide hydrochloride (EDC) and the reaction mixture was stirred for 52 h at room temperature. The resulting solution was extracted with ethyl acetate, and the extract was washed with water and then with a saturated aqueous sodium hydrogen carbonate solution. The organic layer was dried over magnesium sulfate and concentrated, and the residue was dried under high vacuum. This crude product was purified by normal phase column chromatography to give **2** (170 mg, 0.81 mmol) as white solid in 14% yield; mp 185 °C; EI-MS: m/z 210[M]$^+$; ^{1}H NMR (DMSO-d_6, 18 °C): δ 8.65 (q, 1H, -NH-), 8.55 (d, J 8.64 Hz, 1H, H-8), 8.23 (dd, 2H, H-6, H-4), 7.87−7.71 (m, 3H, H-3, H-2, H-7); ^{13}C NMR (DMSO-d_6, 26 °C): δ 168.1 (C=O), 135.9 (C-1), 133.6 (C-6), 131.6 (C-10), 131.3 (C-8), 129.4 (C-9), 128.3 (C-3), 126.7 (C-2), 126.3 (C-7), 125.9 (C-4), 117.5 (CN), 109.2 (C-5), 26.2 (-Me); Anal. Calcd for $C_{13}H_{10}N_2O$: C, 74.27; H, 4.79; N, 13.33%; Found: C, 74.25; H, 4.83; N, 13.04%.

Acknowledgment. This work was supported by a Research Fellowship for Young Scientists (No. 08918) and a Grant-in-Aid for Young Scientists (start-up) (No. 20850023) to G.F., and a Grant-in-Aid for Scientific Research (A) to Y.I. (No. 21245011) from Japan Society for the Promotion of Science, which are gratefully acknowledged. We are grateful to Dr. Toshiko Muneishi for the measurement of 2D-NMR spectra, Prof. Takehiko Wada at Tohoku University for useful discussion, and Dr. Cheng Yang and Ms. Yumi Origane for the assistance in pressure experiments and in the HPLC analyses, respectively.

Supporting Information Available: Instruments and materials used in the present study, reaction scheme and NMR spectra for reference sensitizer **2**, CD spectra of host **1**, fluorescence spectra of **2**, HPLC analyses of **3**, UV−vis spectra of host **1** in the presence of **DPP**, and DFT optimized geometry of **1**. This material is available free of charge via the Internet at http://pubs.acs.org.

(35) (a) Short, W. F.; Wang, H. *J. Chem. Soc.* **1950**, 991. (b) Dewar, M. J. S.; Grisdale, P. J. *J. Chem. Soc.* **1962**, *84*, 35.